JOURNAL OF MATERIALS SCIENCE 3 (1968) 486–497

Crack Formation in Sintered Two-Phase Alloys

H. KELLERER, G. PIATTI
Metallurgy and Ceramics Division, CCR Euratom, Ispra (Varese), Italy

Received 5 March 1968, and in revised form 18 April

Al/Al_2O_3 alloys are characterised by a pronounced high-temperature brittleness which is not yet fully understood. The authors postulated that microcrack formation plays a fundamental role in determining the ductility in tensile and creep tests of these alloys. To investigate the appearance and generation of cracks, density measurements and electron microscope examinations were carried out on samples broken in tensile tests (20 to 620° C temperature range) and in accelerated creep tests (450° C) of two Al/Al_2O_3 alloys (SAP-ISML and Fibroxal). Some investigations were also made on samples deformed by swaging.

The experimental results (morphology, dimensions, distribution and volume of microcracks in the broken samples as a function of temperature and deformation time) confirmed the crack-formation hypothesis and showed that during the deformation of sintered aluminium two-phase alloys, voids may be generated by two mechanisms. The first involves the opening of pre-existing pores which are due to imperfect bonding between matrix and particles, the second involves the creation of new cracks by dislocations blocked at second phase particles.

1. Introduction

The ultimate aim of most of the mechanisms used to strengthen metals is to block dislocation movement. This may be done by increasing the dislocation density so that forest dislocations may stop glide dislocations (work-hardening) or by putting obstacles in the slip planes of the dislocations (precipitation-hardening). If the obstacles are insoluble in the matrix at temperatures close to the melting point (dispersion-hardening), high-temperature strength is obtained.

Unfortunately, most of these strengthening mechanisms reduce ductility. With only a few exceptions, for instance when the matrix itself is brittle [1], dispersion-hardened alloys have lower ductility than the corresponding base metal. Typical examples are the oxide-strengthened aluminium alloys (SAP, XAP, APM, Frittoxal) which have the highest UTS at elevated temperatures (500° C) of all isotropic aluminium alloys, but in which secondary creep-elongation at these temperatures rarely exceeds 0.5%.

It has been found by density measurements [2], optical [3] and electron microscopy [4, 5] of broken Al/Al_2O_3 and Ni/ThO_2 samples that an extremely high number of microporosities are formed in two-phase alloys during deformation. This explains the low ductility of these materials.

This paper is concerned with the formation and appearance of voids formed in Al/Al_2O_3 alloys at temperatures between 20 and 620° C. Voids are supposed to be created mainly by stress concentration at the particle-matrix interface which leads to the opening of cavities in the interface [6]. It has been speculated [2] that in aluminium-based dispersion-hardened alloys, dislocation agglomeration at hard particles should be easier at elevated temperatures. This could explain the increase of cavitation rate and the decrease of ductility with temperature. (*Cavities*, *cracks*, *porosities*, *voids* are used as synonyms throughout the paper.)

2. Experimental

Two types of Al/Al_2O_3 materials were used. Commercial SAP ingots which were obtained from Montecatini and ISML (Italy) and then extruded into bars, and Fibroxal, an alloy which is made from thin aluminium sheets instead of aluminium powder. The fabrication of this material has been described elsewhere [7]. Fabrication conditions and oxide content of these alloys are given in table I.

TABLE I

Alloy	Oxide content (wt %)	Total extrusion ratio
SAP 7%	7.6	150
SAP 7%	7.6	15
Fibroxal A	4.7	14
Fibroxal L	2.5	160

On SAP tensile tests have been made with a 2 ton (1.0 ton $=1.02\times10^3$ kg) hydraulic Losenhausen apparatus. The samples had a gauge length of 5 cm at a diameter of 10 mm. Small pieces were cut from the tensile specimens for metallographic evaluation and for density measurements.

Fibroxal bars have been swaged at room temperature from diameters of 19 to 3 mm. No intermediate heat-treatments were used. Electron micrographs were made with a two-stage replica technique and the photographs were taken on a Philips electron microscope at 100 KV. The density values were measured by the immersion technique, with tetrachlorethyl as immersion liquid. Depending on the procedure employed, precision varied for the various measurements. The estimated error is approximately ±0.002 g/cm^3 for samples taken in the rupture zones, and below ±0.001 g/cm^3 for the other samples.

3. Results

3.1. Void Distribution in Broken Samples

The crack distribution in broken samples of SAP 7% may be seen from the micrographs in figs. 1, 2, 3. The samples are unetched so that the oxide is scarcely visible. Three test temperatures were chosen: 20, 450, and 620° C. For each temperature the structure is shown immediately at the rupture surface and at approximately 4 mm from the fracture surface. Several facts may be seen from these, and other optical micrographs. (i) The number of cracks per unit surface increases with the test temperature.

Figure 1 Aspect of SAP specimen ruptured at 20° C; rupture zone (× 90).

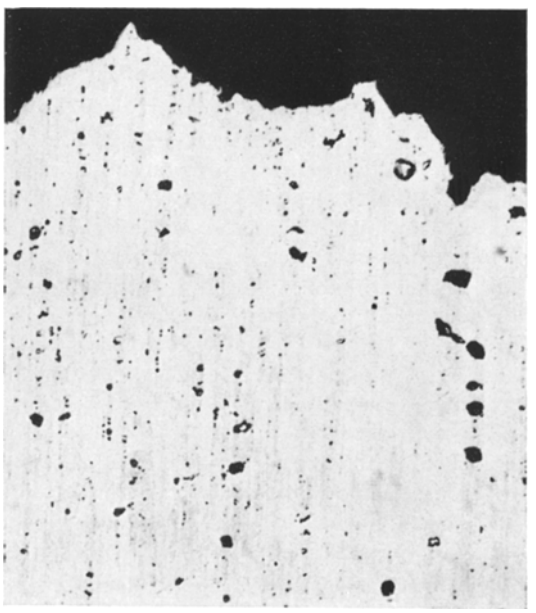

Figure 2 Aspect of SAP specimen ruptured at 450° C; rupture zone (× 90).

(ii) The number of cracks and their dimensions decrease as the distance from the fracture surface increases. (iii) Cracks are often aligned in lines parallel to the specimen axis and are most likely to be situated in oxide-rich zones. (iv) Near

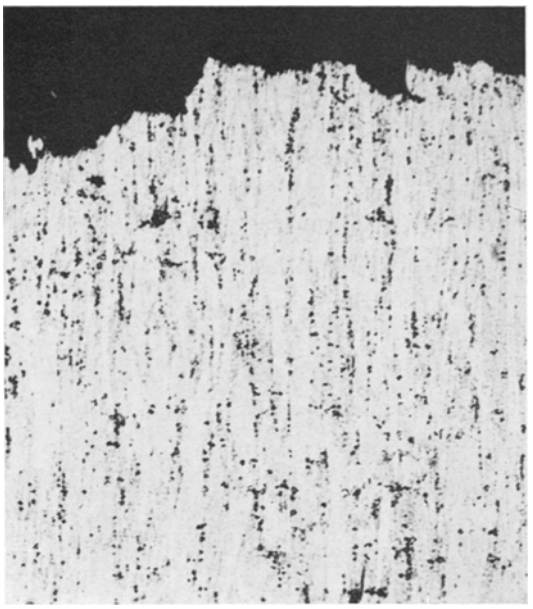

Figure 3 Aspect of SAP specimen ruptured at 620° C; rupture zone (× 90).

the fracture surfaces the linear dimensions of the porosities may reach 100 μm. (v) The examination of transversal surfaces shows that cavities are uniformly distributed over the specimen and have approximately the same dimensions in the other two directions.

In the specimens broken at 20° C, long cracks at an angle of 45° to the tensile axis are often seen; these transverse the longitudinal oxide stringers which are typical for SAP. (Some of these cracks are visible in fig. 1.) The examination of a specimen exhibiting unusually low ductility showed that in this case not the amount but the length of these 45°-cracks was drastically increased. This may explain the marked effect which oxide-banding has on ductility. As on the other hand extrusion is, in part, responsible for these stringers, the influence of the extrusion conditions seems to be important.

A specimen broken at −196° C has been included in these investigations but no cracks could be seen under the optical microscope even at high magnifications and fractographs show ductile fracture. The influence of temperature on crack formation is therefore quite evident.

3.2. Form and Appearance of Voids

Electron micrographs were made from the ruptured specimens to show the appearance of the cavities. The carbon-replica technique was used to facilitate comparison with other investigations. As it is assumed from previous work that SAP does not have the theoretical density [2], the as-extruded material has also been checked.

Figure 4 Microporosities in as-extruded SAP (× 20000).

3.2.1. As-extruded SAP

Fig. 4 illustrates irregularities which are thought to be micro-porosities in the as-extruded material. It was found that they can be seen more easily in sections normal to the extrusion axis than in those parallel to it. Typically one finds circular porosities encompassing an area of about 1 to 5 μm. As the starting powder for the fabrication of SAP alloys has average diameters of about 40 μm, these are probably not the contours of badly sintered particles but sintering defects inside the particles. As this may be of importance, the present results and considerations are to be regarded as valid mainly for sintered materials which exhibit these defects.

3.2.2. Broken Specimens

The information already gained by the optical microscopy are confirmed by the electron micrographs of the broken samples. Typical pictures are shown in figs. 5 to 7. The main

(a)

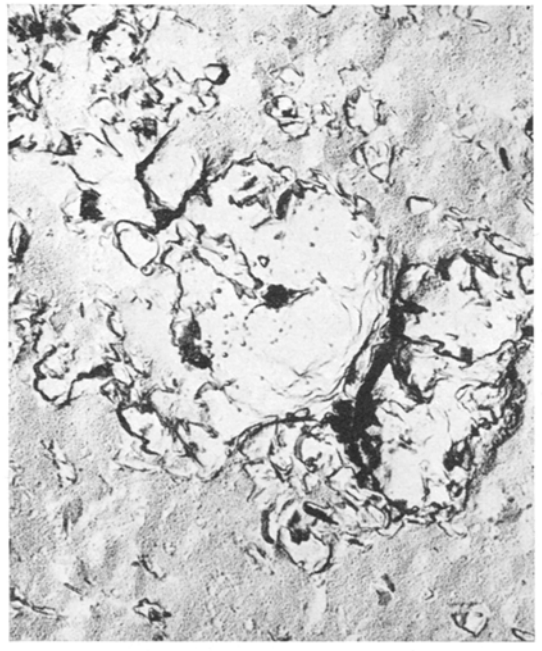

(b)

Figure 5a, b Microcracks found in SAP specimen ruptured at 20° C (× 20000).

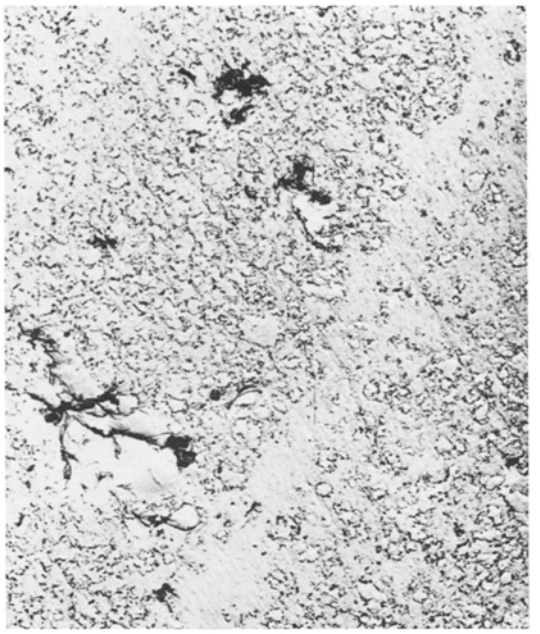

(a)

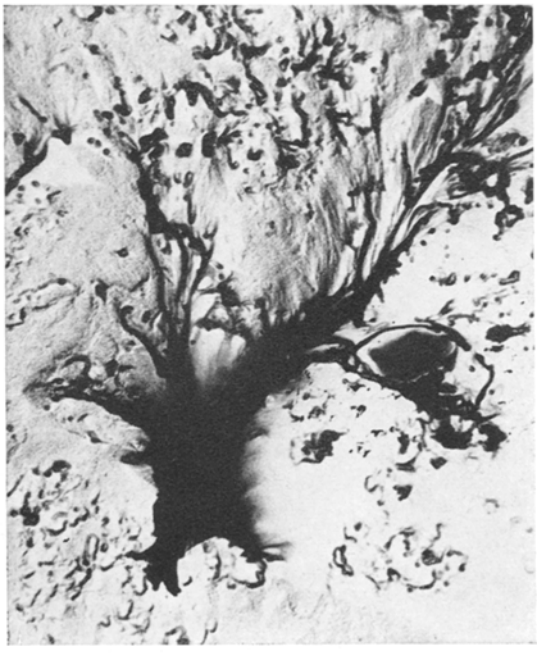

(b)

Figure 6 Microcracks found in SAP specimen ruptured at 450° C; (a) × 3000, (b) × 20000.

difference between deformation at 20° C and at 450° C is that the long 45°-cracks appear only at room temperature, but very large round cracks are formed at 450°. The general appearance of the voids does not change very much.

Typical examples both from near the fracture

(a)

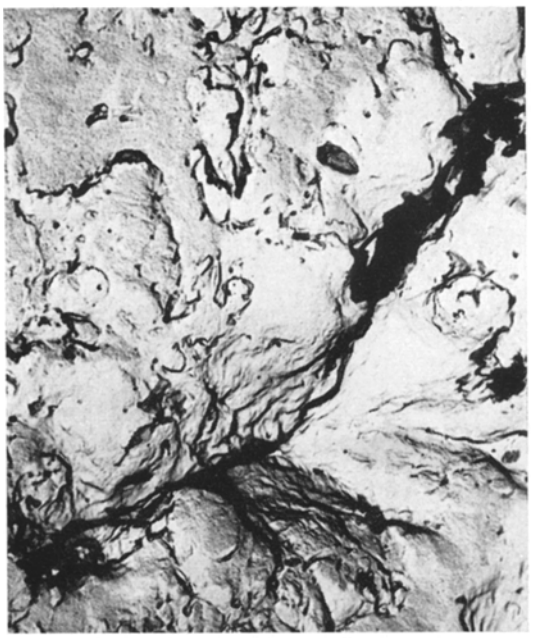

(b)

Figure 7 Microcracks found in SAP specimen ruptured at 620° C; (a) × 3000, (b) × 20000.

surface and from points at some distance from it are given in fig. 6. They permit the following conclusions to be drawn. (i) It is evident that cracks originate and are concentrated near the oxide particles and are frequently stopped when approaching aluminium zones. This fact can be attributed to the plastic deformation which is possible in the aluminium matrix. (ii) Crack tips are usually very sharp. This evidently leads to high stress concentrations at the tip and facilitates crack propagation. (iii) Two types of cavities can clearly be distinguished: one is roughly circular-shaped, similar to those seen in the as-extruded specimens. Typical examples are shown in fig. 6a. Long and narrow cracks, apparently often created by the combination of several smaller porosities, are shown in fig. 6b. Sometimes a complicated network of cracks around one major void is found. (iv) Except in the actual zone of fracture, crack length (under the present conditions of observation) rarely exceeds 10 to 20 μm. Most of the visible cavities are in the 1 μm range.

It is difficult to make exact statements, however, since the sample preparation and the resolution of the microscope have to be taken into consideration.

The picture changes somewhat for the specimens broken at 620° C. It may be seen from figs. 3 and 7 that more porosities are present, both in the rupture zone and at some distance from it. The average volume of most voids remains constant but it seems that in the 620° C specimen, fewer very large cracks are found than in the 450° C sample. Void appearance, also, changes. Wedge-shaped cracks are often encountered together with the long, narrow cracks. The circular voids which seemed to surround undamaged areas in the other samples appear now as agglomerations of holes.

3.3. Void Volume

Giarda and Paganelli [4] have made measurements of crack frequency on electron micrographs and calculated the average number of cracks per surface unit. As this permits only local measurements, an integrating method for the measurement of the cracks was used by determining the specific weight of the material. This system has been employed by Boettner and Robertson [8] for the determination of microvoids in copper. Figs. 1 to 3 show that there is a gradient in crack-density over the length of the sample, at least near the rupture surface. The total density of the material will therefore depend on the volume of the specimen. This fact has been confirmed by a series of density

measurements carried out on a single broken sample. After each measurement, the size of the sample was reduced by sawing slices off the side opposite the fracture. The results are shown in fig. 8. The diagram suggests that total crack volume, V_c depends on the distance from the fracture surface, a, according to an equation $V_c = A - B \ln a$ for the short region investigated.

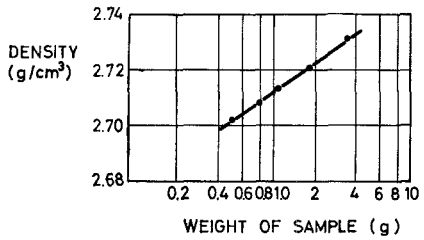

Figure 8 Density of the rupture zone of a SAP specimen ruptured at 450° C plotted against specimen weight.

To compare ruptured samples with each other a standard weight of 1.5 g was used. Tensile specimens were broken at temperatures between 20 and 620° C. The density of the rupture zones (i.e. necked zones) is plotted in fig. 9. A steady decrease of the density with test temperature is seen, reflecting the high degree of void

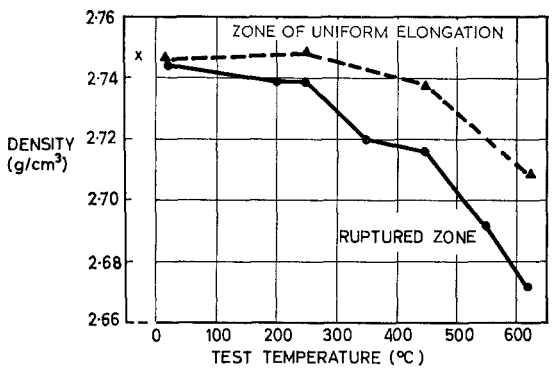

Figure 9 Density of rupture zones and zones of uniform elongation of SAP extruded with a ratio of 1:15, plotted against temperature of rupture.

formation during tensile deformation at elevated temperatures, especially above 300° C. The broken line indicates the density of the zone of uniform elongation where strain is smaller. Except for the specimen tested at 620° C, it has been shown clearly that a considerable number of voids are formed in the necked region only.

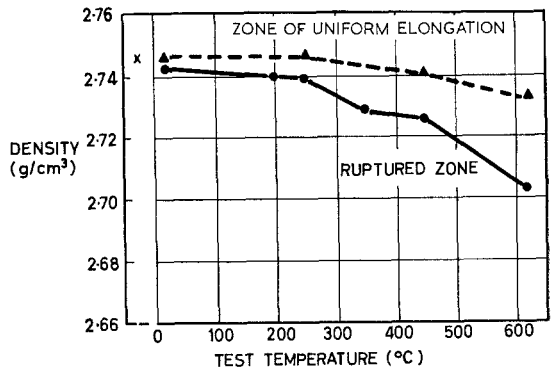

Figure 10 Density of rupture zones and zones of uniform elongation of SAP extruded with a ratio of 1:150, plotted against temperature of rupture.

A slight increase in density at 250° C, which has been found on several occasions, is attributed to measurement dispersion. It may be noted, however, that during light deformation of aluminium very small density increases are possible owing to the disappearance of vacancies [9].

If part of the cavities were due to pre-existing porosities in the material, they will be somewhat influenced by the fabrication method. This was investigated by measuring the density of a SAP material obtained from a different manufacturer and extruded (in two steps) with a ten-fold extrusion ratio. The corresponding results are illustrated in fig. 10, where a marked difference from fig. 9 can be seen. We think that with the more pronounced deformation due to the high extrusion ratio, fewer microporosities are existent in the as-extruded material and a better contact is established between the oxide and the matrix. This should lead to a decreased rate of crack formation during subsequent tensile testing. A connexion has previously been discovered between fabrication schedule on one side and strength and ductility on the other [4]. The micrographs shown in figs. 1 to 3 permit the conclusion that the increased total void volume at elevated temperature is not due to larger porosities, but to a greater number of them than at 20° C. This is consistent with the hypothesis that part of the cavities already exist in the as-extruded material and that their apparent number is partly determined by the growth of sub-microscopic cavities until they become visible. One can accept the concept of Gilbert *et al* [1] who speak of built-in cracks as

consisting of crack surfaces physically in contact but not bonded to each other. These cracks can then open during deformation.

3.4. Void Formation

It is evident from the preceding diagrams that void volume at a given point of a tensile specimen depends on deformation at this point. This allows the rate of void formation to be followed by measuring the density as a function of local strain. Little information will be gained from specimens deformed at 20° C as few voids are formed. The rupture-process at 450° C was therefore investigated. Samples have been deformed to total plastic elongations (over the entire gauge length) between 0.5 and 6%. Two nominal initial loading speeds of 0.023 kg/mm² sec and 0.057 kg/mm² sec were used. Small samples for density measurements were then taken from the deformed specimens, each sample with a different reduction in area. Contrary to the method indicated for figs. 9 and 10, no standard weight was fixed, but samples are characterised by reduction in area. As most pieces were conical, however, two values of reduction in area have to be attributed to each sample. Therefore, instead of unique values of deformation, zones are indicated in fig. 11, which summarises the results obtained on ten broken or non-broken tensile specimens. (Some specimens provided serial samples.) Local density values are shown as a function of local reduction in area for two deformation speeds, at the same temperature.

The following conclusions may be drawn from this diagram. (i) Higher deformation speed leads to a reduced rate of void formation, in the initial 3% reduction in area. These findings are emphasised by the shape of the "creep curve". (ii) After the initial density decrease, void formation proceeds more slowly and the difference in slope between the two curves gets smaller. (iii) Void formation rate increases again immediately prior to rupture. (iv) The dispersion of the results, especially at low deformations, is surprisingly small, given the large amount of inhomogeneities present in the sintered aluminium alloys.

To get further information on the influence of deformation speed, very fast time-to-rupture tests at constant load were performed on the same material. Care was taken to remain in the zone where no reversal phenomena take place [2].

The results for two tests are plotted in fig. 12. It is easily seen that the trend indicated by the tensile tests is maintained in the fast "creep"

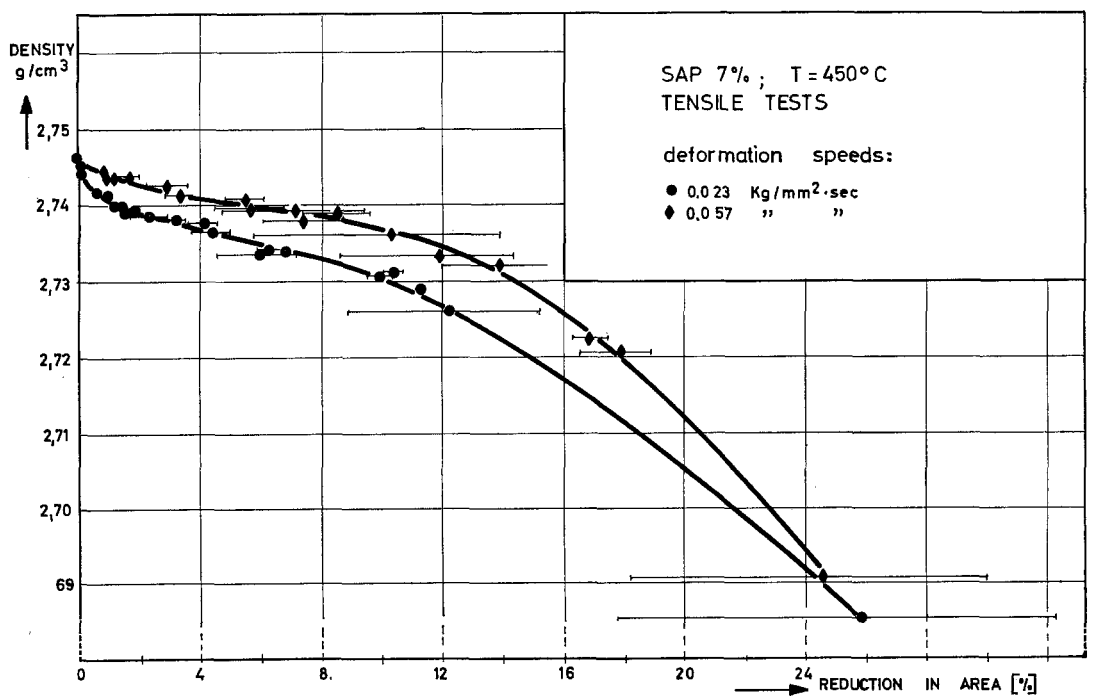

Figure 11 Density of SAP strained by tensile deformation at 450° C plotted against reduction in area.

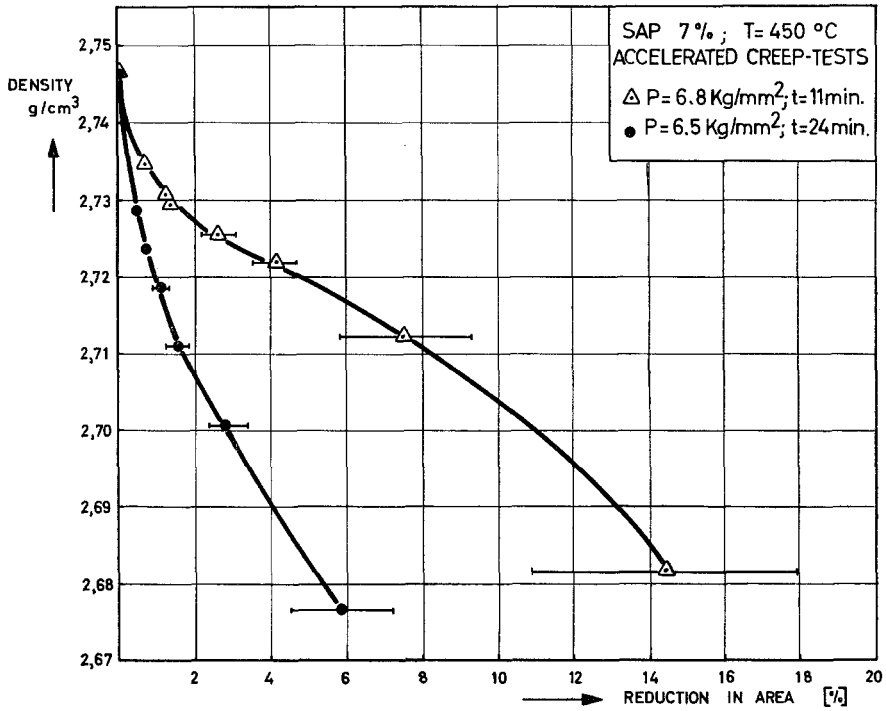

Figure 12 Density of SAP 7% specimens stressed by accelerated creep-test.

tests, that is, crack formation increases with time to rupture. This corresponds to the results reported in the literature on copper. It is seen that the aspect of the curves changes gradually with decreasing load (which corresponds to increasing time to rupture), the "plateau" which appears in the tensile curves and which is still visible in the 11 min test of fig. 12 disappears completely at a life-time of 24 min. The behaviour at still longer times to rupture will be discussed in a separate paper [10].

The fact that many submicroscopical voids are obviously already formed at reduction in areas as small as 1% is difficult to explain by the formation of new porosities alone. It may be thought to be due to the opening of the pre-existing voids in the matrix. This leads to separations in the specimen which afterwards are opened and connected by tearing and by the appearance of newly formed cracks.

An inflection point beyond which crack-formation increases again may be seen in fig. 11 at deformations around 12%. This corresponds to the region where cracks begin to become visible in the light microscope.

3.5. Voids Formed by Swaging

In the previous section we have considered void formation mainly in the oxide-aluminium interface either by opening of existing cavities or by breaking of this interface. A certain measure of propagation of the cracks into the matrix is also possible.

It has been tacitly assumed that no deformation of the second phase takes place. This is the basis of most dispersion-hardening theories. An exception is the model of Ansell and Lenel, who assume that the rate-controlling process is the breaking of oxide particles [11]. This however, has never been observed in commercial SAP. Ashby [6] shows in his analysis of cavitation around hard second-phase particles that rupture of the hard particles in a ductile matrix should only occur for very large particle sizes. To investigate the effect of particle deformation, an alloy with a coarser dispersion had to be used.

As the Fibroxal alloys permit large variations in particle size [12], some deformation experiments were carried out on this material. Tensile tests permit only limited amounts of reduction in area. Circular swaging has therefore been chosen and work-hardening was controlled by subsequent tensile tests and hardness measurements [12]. A typical example is shown in fig. 13a. The behaviour of 99.5% Al is depicted for comparison

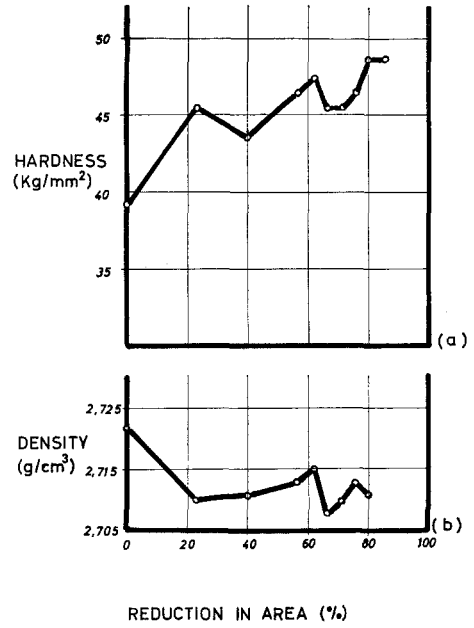

Figure 13 Hardness and density of Fibroxal deformed by swaging plotted against reduction in area.

in fig. 14a. A large amount of "work-softening" was found for all Fibroxal alloys with oxide contents $> 0.5\%$ at approximately 30% reduction in area and sometimes again at approximately 80%. Similar irregularities in the behaviour of two-phase alloys have already been quoted in the literature, for instance for Al/Ag [13] or Cu/In [14]. A literature survey is given by Doennges [15].

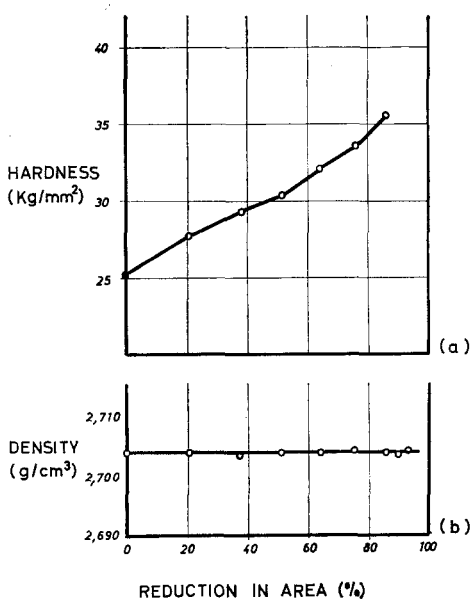

Figure 14 Hardness and density of aluminium deformed by swaging plotted against reduction in area.

Different explanations have been offered, for instance reorientation of the second phase [13] or Bauschinger effects [16]. Borchers *et al* [7, 17] have suggested that the phenomena could be due to extensive creation of microporosities in the material, which would reduce hardness and tensile strength. This theory can be proved by density measurements. Fig. 13b shows effectively large variations in the density of the two-phase alloy during swaging, whilst the aluminium sample in fig. 14b remains almost constant. However, the deformation leads to the breaking of the large oxide platelets and reorientation of the dispersed phase. This is obvious from the sequence of micrographs in fig. 15 which illustrates the microstructures at various degrees of deformation. It can be imagined that new oxide/aluminium, aluminium/aluminium and to a lesser extent oxide/oxide surfaces must be formed during this process and this should favour the appearance of porosities. As an increase in density and hardness is often found in the later stages of deformation, porosities can eventually be rewelded and sintered. There is some evidence that this occurs mainly in fine dispersions. Recrystallisation experiments show that annealing is not sufficient to close the porosities. Samples deformed in the "critical zones" retain lower strength as compared to those swaged to other degrees even after heat-treatments.

4. Discussion

The findings presented above show that during the deformation of sintered aluminium two-phase alloys between 20 and 620° C voids may be generated by the following three mechanisms. (i) Opening of pre-existing porosities which are due to imperfect sintering. (ii) Creation of new cracks by dislocations blocked at second phase particles. (iii) Breaking and rearrangement of large particles which leads to the creation of new interfaces. A fourth mechanism for the formation of porosities probably exists by accumulation of trapped gases forming bubbles. This has been found during high-temperature thermal cycling [3]. During tensile deformation of SAP mainly the two first mechanisms may be important. The increased crack formation at high temperature has been explained by easier dislocation pile-up followed by cavitation by a

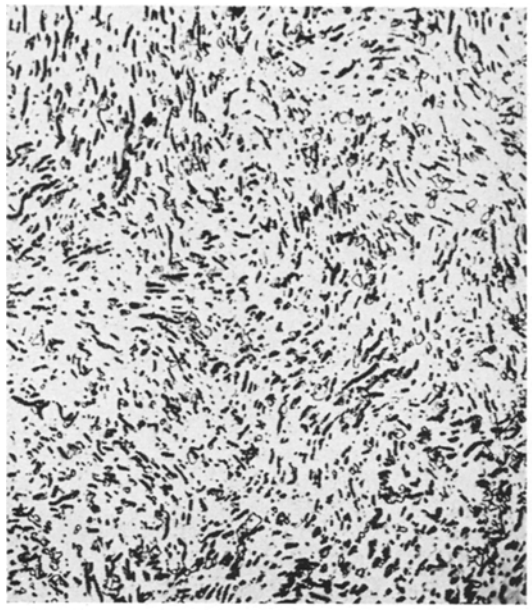

(a)

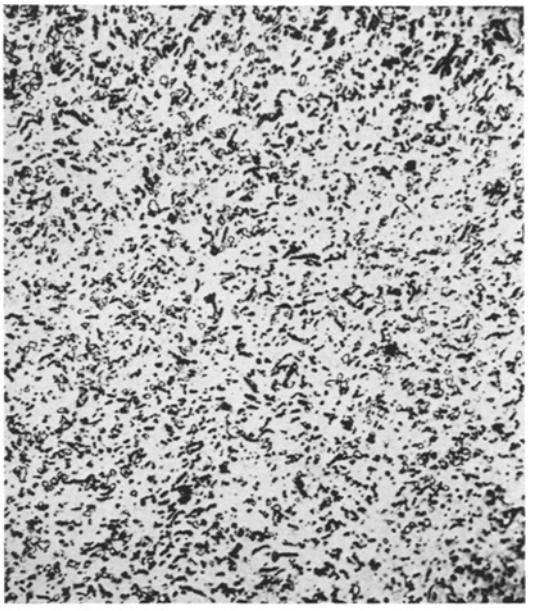

(b)

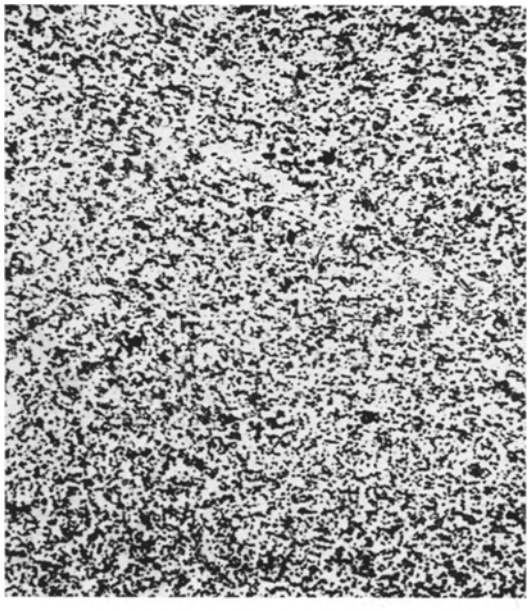

(c)

Figure 15 Breaking of oxide particles in Fibroxal A during deformation by swaging (× 500); (a) as-extruded, (b) swaged 45%, (c) swaged 85%.

Griffith mechanism [2]. It seems that the opening of pre-existing cracks or badly bonded surfaces, too, is temperature- and time-dependent. This encourages one to think in terms of a viscous behaviour of these crack interfaces.

It is evident that void formation should have a considerable effect on the mechanical properties on ultimate tensile strength, uniform elongation and total plastic strain. To consider these consequences, one may depart from the assumption that most of the cracks start somewhere at an oxide/aluminium interface. If the bonding between the oxide and the aluminium is weakened the influence of the oxide on the mechanical properties of the composite should also decrease, and the SAP-characteristics should tend towards those of a pure aluminium with a large amount of holes.

For the strength of the material this is shown to be true in fig. 13, where minima of density mostly correspond to minima of hardness. It is difficult to determine how crack formation influences tensile strength, but it is known, however, that SAP alloys which have more cracks in the as-extruded state are less strong. Elevated testing rates (e.g. up to 1 cm/min) at 450° C give higher strength as well as higher elongation, and there may be a connexion between this and the fact (evident in fig. 11) that at these elevated rates fewer microcracks are created.

At elevated test temperatures considerable void volumes have already formed at very small strains (fig. 11). Consequently, high local void concentrations are already possible at low deformation values. The chances for early

necking are therefore increased as the load-supporting area is diminished. This explains why the uniform elongation of SAP decreases sharply with increasing testing temperature, as shown in fig. 16, and arrives at extremely low values of less than 1% in just the temperature region where, according to figs. 9 and 10, crack formation begins to be important.

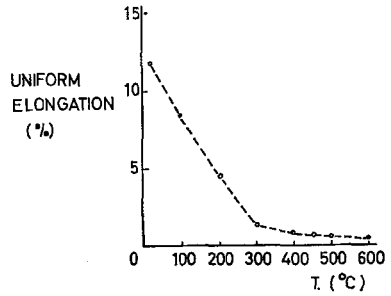

Figure 16 Uniform elongation of SAP 7% as a function of test temperature.

Ashby [5] states that cavitation by blocked dislocations should occur earlier in specimens containing more closely spaced particles. One could expect therefore, for SAP to have a cavitation rate which increases with oxide content, as this leads in time to a reduced interparticle spacing. However, no great variations in density decrease with oxide content have been found [2]. This is thought to be due to two factors: SAP with higher Al_2O_3 content contains smaller particles and can therefore be strained further without cavitations than one containing bigger particles (when only the formation of new cracks is considered [5]). On the other hand, with decreasing the interparticle spacing the flow stress increases. As it has been shown that dislocation density increases linearly with flow stress [18], the number of dislocations available between obstacles for crack formation will not change very much with oxide content, if a certain minimum value of the oxide content is passed. In the Fibroxal-alloy range oxide contents as low as 0.1% were investigated and a dependence of uniform elongation on oxide content was found only for alloys containing less than 2% Al_2O_3. This is shown in fig. 17. Above this critical value uniform elongation hardly changes with oxide content and remains alike for both SAP and Fibroxal alloys.

The situation changes if total plastic strain is considered. It is thought that this depends to a

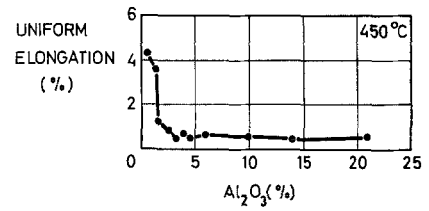

Figure 17 Uniform elongation of different SAP and Fibroxal alloys deformed at 350° C plotted against oxide content.

large extent on the fact that many of the strengthening and embrittling oxide particles are now separated from the matrix and are therefore ineffective. The "aluminium-bridges" between the oxide layers should now be able to neck down and give local ductile fracture combined with some elongation.

This has recently been confirmed by electron-fractographs of SAP samples broken at different temperatures [19]. The fracture surfaces show many regions broken by ductile shearing. This leads one to the conclusion that crack formation in the sintered aluminium/oxide alloys always leads to decreased uniform elongation, but may have some beneficial influence on total plastic elongation.

5. Conclusions

1. Density measurements and electron microscope examinations (replica) were carried out on samples of sintered aluminium two-phase alloys, Al/Al_2O_3, broken in tensile tests (20 to 620° C temperature range) and accelerated creep tests (450° C).
2. Both experimental techniques gave evidence of the presence of microcracks whose formation is a function of temperature and deformation rates during mechanical tests.
3. The voids seem to be generated during deformation by two probable mechanisms: opening of pre-existing porosities which are due to imperfectly bonded Al/Al_2O_3 interfaces and creation of new cracks by dislocations piled up at Al_2O_3 particles.
4. The high rate of crack-formation during deformation in sintered aluminium two-phase alloys explains the low ductility of these materials at high temperatures.

Acknowledgements

We thank Mr Wolter, Berlin, for many density measurements and Mr Finet, Ispra, for the micrographs. We are very grateful to Dr H. W.

Schleicher for many stimulating discussions during the course of this investigation.

References

1. A. GILBERT, J. L. RATLIFF, and W. R. WARKE, *Trans. ASM* **58** (1965) 142.
2. H. KELLERER and G. PIATTI, *J. Materials. Sci.* **3** (1968) 222.
3. G. BEGHI, P. GUYOT, and G. PIATTI, *Mém. Sci. Rev. Mét.* **61** (1964) 191.
4. A. GIARDA, and M. PAGANELLI, *ibid* **62** (1965) 921.
5. B. A. WILCOX and A. M. CLAUER, *Trans. Met. Soc. AIME* **233** (1965) 253.
6. M. F. ASHBY, *Phil. Mag.* **14** (1966) 1157.
7. H. BORCHERS, G. SAUR, and H. KELLERER, *Aluminium* **44** (1968) 102.
8. R. C. BOETTNER and W. P. ROBERTSON, *Trans. Met. Soc. AIME* **221** (1961) 613.
9. K. SEKAZI and D. KUHLMANN-WILSDORF, *Acta Met.* **14** (1966) 1131.
10. P. BONNET, H. KELLERER, and G. PIATTI, to be presented at Powder Metallurgy Symposium Stuttgart, 1968.
11. G. S. ANSELL and F. V. LENEL, *Acta Met.* **8** (1960) 612.
12. H. KELLERER, G. SAUR, and H. BORCHERS, Euratom Report EUR 3497 (1967).
13. G. PYSZ, *Neue Hütte* **10** (1965) 683.
14. H. BÖMM, *Z. Metallk.* **54** (1963) 224.
15. E. DOENNGES, *ibid* **46** (1965) 867.
16. N. H. POLAKOWSKI, *J. Iron Steel Inst.* **169** (1951) 337.
17. H. BORCHERS and W. SCHARFENBERGER, *Metallwirtschaft* **20** (1966) 805.
18. P. SCHILLER, *Mém. Sci. Rev. Mét.* **9** (1967) 791.
19. D. G. HARMAN and T. A. NOLAN, Oak Ridge (USA) Report ORNL TM 1826 (1967).